12. C. R. Bina and B. J. Wood, *ibid.*, p. 955; T. Irifune, T. Sekine, A. E. Ringwood, W. O. Hibberson, *Earth Planet. Sci. Lett.* **77**, 245 (1986).
13. Stishovite, the ultrahigh pressure form of quartz (SiO_2), has Si in octahedral coordination, which is the case also for majorite and other garnet-structured pyroxenes.
14. The formulas of the low-pressure pyroxenes, enstatite ($MgSiO_3$), diopside ($CaMgSi_2O_6$), and jadeite ($NaAlSi_2O_6$) may be recast into high-pressure garnets such that enstatite is $Mg_4Si_4O_{12}$, diopside is $Ca_2Mg_2Si_4O_{12}$, and jadeite is $Na_2Al_2Si_4O_{12}$. The Si:O ratio is 4:12, in contrast to pyrope garnet, for example, which is 3:12 ($Mg_3Al_2Si_3O_{12}$). Some upper mantle pyroxenes contain a Ca-Tschermak ($CaAl_2SiO_6$) molecule in solid solution and thus have Al^{IV} and Al^{VI}. Aluminum in tetrahedral coordination is negligible above 100 kbar, so that the high-pressure transformation of Ca-Ts to garnet is similar to the transformation of other low-pressure pyroxenes in which some Si becomes octahedrally coordinated (*15*).
15. H. Yamada and E. Takahashi, in *Proceedings of the Third Kimberlite Conference*, J. Kornprobst, Ed. (Elsevier, Amsterdam, 1984), vol. 2, pp. 247–255.
16. A. E. Ringwood and A. Major, *Earth Planet. Sci. Lett.* **1**, 351 (1966); A. E. Ringwood, *ibid.* **2**, 255 (1967).
17. R. O. Moore and J. J. Gurney, *Nature* **318**, 553 (1985).
18. M. C. Wilding, B. Harte, J. W. Harris, paper presented at the 28th International Geologic Congress, 9 to 19 July 1989, Washington, DC, abstr. vol. 3, p. 359.
19. Jagersfontein is close to the edge of Kaapvaal Craton and is the site where the connection between diamonds and kimberlites was first made. It is the source of the standard end-member blue-white diamond.
20. S. Andersson and M. O'Keeffe, *Nature* **267**, 605 (1977).
21. J. V. Walther and B. J. Wood, *Contrib. Mineral. Petrol.* **88**, 246 (1984); D. M. Carmichael, *ibid.* **20**, 244 (1969); V. Sautter, O. Jaoul, F. Abel, *Earth Planet. Sci. Lett.* **89**, 109 (1988).
22. A JEOL microprobe was used for analysis of JX-25 and a CAMECA with a different set of standards for JX-50.
23. H. Tsai, H. O. A. Meyer, J. Moreau, H. J. Milledge, *Proceedings of the Second Kimberlite Conference*, F. R. Boyd and H. O. A. Meyer, Eds. (American Geophysical Union, Washington, DC, 1979), vol. 1, pp. 16–26.
24. End-member zero-pressure densities used in calculating the reconstituted garnet compositions in Table 2 were taken from G. R. Johnson and G. R. Olhoeft, in *Handbook of Physical Properties of Rocks*, R. S. Carmichael, Ed. (Chemical Rubber Company, Boca Raton, FL, 1984), vol. 3, pp. 1–38. Calculated densities are JX-25 garnet, 3.68 g/cm^3; clinopyroxene, 3.27 g/cm^3; JX-50 garnet, 3.71 g/cm^3; clinopyroxene, 3.14 g/cm^3.
25. M. Akaogi and S. Akimoto, *Phys. Chem. Planet. Inter.* **15**, 90 (1977); L. Liu, *Earth Planet. Sci. Lett.* **36**, 237 (1977).
26. M. Akaogi and S. Akimoto, *Phys. Earth Planet. Inter.* **19**, 31 (1979).
27. T. Gasparik, *Contrib. Mineral. Petrol.* **102**, 389 (1989).
28. T. Irifune and A. E. Ringwood, *Earth Planet. Sci. Lett.* **86**, 365 (1987); T. Irifune, *Phys. Earth Planet. Inter.* **45**, 324 (1987).
29. Akaogi and Akimoto (*26*) also studied the system ferrosilite ($Fe_4Si_4O_{12}$)–almandine ($Fe_3Al_2Si_3O_{12}$) and showed that Fe-rich pyroxene solid solution in garnet behaves in much the same way as in the analog MAS system.
30. T. Sekine *et al.*, *Nature* **319**, 584 (1986).
31. D. J. Ellis and D. H. Green, *Contrib. Mineral. Petrol.* **71**, 13 (1979).
32. I. D. MacGregor and W. I. Manton, *J. Geophys. Res.* **91**, 14,079 (1986). Sample R-1A reported by these authors is similar to JX-25 and JX-50.
33. D. V. Hills and S. E. Haggerty, *Contrib. Mineral. Petrol.* **103**, 397 (1989). Sample KEC 86-8 is probably of ultradeep origin.
34. J. W. Shervais *et al.*, *Geol. Soc. Am. Bull.* **100**, 411 (1988). Sample 437-1 is similar to JX-25 and JX-50.
35. H. O. A. Meyer, in (*1*), pp. 501–522.
36. S. H. Richardson, J. J. Gurney, A. J. Erlank, J. W. Harris, *Nature* **310**, 198 (1984); S. H. Richardson, *ibid.* **322**, 623.
37. We thank the DeBeers Mining Company for access to Jagersfontein and their logistical support. Assistance with the electron microprobe analyses was provided by S. Field and O. Soncini. We acknowledge the detailed comments by S. A. Morse, H. W. Jaffe, T. Gasparik, L. W. Finger, D. L. Anderson, M. Williams, and three anonymous reviewers. We thank the National Science Foundation for support under grant EAR89-05046 (to S.E.H.); the University of Massachusetts for a faculty fellowship (to S.E.H.); and the Centre National de la Recherche for a grant from the INSU-DBT program, Theme 4: Fluids, minerals and kinetics (to V.S.). Contribution 159.

20 February 1990; accepted 24 April 1990

Increase in the Stratospheric Background Sulfuric Acid Aerosol Mass in the Past 10 Years

D. J. HOFMANN

Data obtained from measurements of the stratospheric aerosol at Laramie, Wyoming (41°N), indicate that the background or nonvolcanic stratospheric sulfuric acid aerosol mass at northern mid-latitudes has increased by about 5 ± 2 percent per year during the past 10 years. Whether this increase is natural or anthropogenic could not be determined at this time because of inadequate information on sulfur sources, in particular, carbonyl sulfide, which is thought to be the dominant nonvolcanic source of stratospheric sulfuric acid vapor. An increase in stratospheric sulfate levels has important climatic implications as well as heterogeneous chemical effects that may alter the concentration of stratospheric ozone.

THE DOMINANT SOURCE OF SULFURIC acid (H_2SO_4) aerosol in the stratosphere is major volcanic eruptions that impulsively inject sulfur dioxide (SO_2) to altitudes of 20 to 25 km; this SO_2 subsequently forms H_2SO_4 vapor, which is followed by aerosol nucleation and growth. The physical state of the stratospheric aerosol is an aqueous spherical droplet composed of 60 to 80% sulfuric acid for temperatures from −80° to −45°C, respectively (*1*). In 1959, Junge *et al.* (*2*) showed by direct observations through particle impactor measurements that a stable layer of sulfur-containing aerosol particles persists in the stratosphere, albeit at a low level, even during periods without major, tropopause-penetrating volcanic eruptions. Ambient levels of SO_2 in the upper troposphere and stratosphere are low because of its reactivity and water solubility and are not believed capable of producing this natural background. Crutzen (*3*) suggested that a sulfur-bearing compound that is chemically inert and water-insoluble, such as carbonyl sulfide (OCS), may instead be responsible. In this model, OCS diffuses into the stratosphere, where it is dissociated by solar ultraviolet radiation and eventually forms sulfuric acid. Measurements of stratospheric OCS concentrations (*4, 5*) and results of detailed chemical and dynamical modeling studies (*6, 7*) are in general agreement with this dissociation hypothesis. Carbon disulfide (CS_2), which is probably converted to OCS in the troposphere, may also be important. Because it is estimated that up to 25% of the atmospheric burden of these sulfur compounds are by-products of biomass burning, fossil-fuel burning, petroleum refining, and other industrial processes, their atmospheric levels should be increasing. Although there have not been any long-term studies of OCS concentrations in the stratosphere, this gas appears to have been present at the 500 pptv (parts per trillion by volume) level since at least 1976 (*8*).

Problems associated with an increasing sulfuric acid layer in the stratosphere are numerous. In addition to climate considerations, heterogeneous chemical conversion of inactive forms of chlorine by aerosols containing sulfuric acid and water is now thought to be important in stratospheric ozone depletion after major volcanic eruptions (*9*). Increased scattered solar radiation will alter photochemistry and may even accelerate the conversion of OCS to H_2SO_4. Because the aerosol uses up water both in the conversion of OCS and in aerosol formation, it is a sink for H_2O and may play a role in dehydration of the stratosphere, although this effect is expected to be small because of the relative mixing ratios involved.

Balloon soundings over Laramie, Wyoming (41°N), where the vertical distribution of atmospheric aerosols is measured approximately monthly with optical particle counters (*10*), were analyzed for the period

---

Department of Physics and Astronomy, University of Wyoming, Laramie, WY 82071.

1979 to 1990 and compared with results of earlier studies to evaluate whether the atmospheric levels have increased recently. The measurements by Junge *et al.*, in 1959, were made near the end of an extended volcanic eruption–free period that was terminated by the eruption of Agung in the Southern Hemisphere in 1963. Measured aerosol concentrations were about 0.1 cm^{-3} for radii greater than about 0.15 μm. Measurements at Laramie, begun in 1971, indicated stable concentrations of about 0.5 cm^{-3} for this size range during a nonvolcanic period from mid-1978 through 1979. Comparison of these data suggested that there had been an increase of 9 ± 2% per year or a doubling time of about 8 years, if the increase had occurred exponentially (*11, 12*). However, because different techniques were used in obtaining the two data sets, there was considerable doubt about this hypothesized increase.

Since the eruption of El Chichon in Mexico in 1982, only the comparatively minor eruption of Nevado del Ruiz, in Colombia, in late 1985 appears to have disturbed the stratosphere. The eruptions of Santiaguito, in Guatemala, in mid-1989 had only minor effects in the lower stratosphere (*13*), and the recent eruptions of Remount, in Alaska, have not disturbed the 20-km aerosol level at Laramie as of February 1990. Since late 1988, 20-km aerosol levels at Laramie have remained relatively constant. In the polar regions, they appear to have changed little since 1986. Volcanic eruptions capable of injecting SO_2 to 15 to 20 km seldom go unnoticed; they are usually detected in satellite imagery, solar extinction measurements, and twilight observations (if not observed directly). Minor volcanic eruptions and fumaroles do not contribute to the stratospheric burden because OCS is a trace volcanic effluent and volcanic SO_2 from these sources does not penetrate the tropopause. It is unlikely that a constant stratospheric aerosol level is due to numerous small unobserved eruptions. The current background status of the stratospheric aerosol layer affords one the opportunity to compare such levels 10 years apart, using the same measurement and instrument calibration technique, to evaluate whether they have increased recently.

About 250 balloon soundings to measure the aerosol concentration or mixing ratio at the stratospheric maximum, which normally occurs in the altitude range from 18 to 22 km, have been made at Laramie since 1971 (Fig. 1). Large aerosol increases caused by volcanic eruptions are obvious. These eruptions generally, although not always, increase the average particle size, resulting in a decrease in the ratio of the two size ranges measured (Fig. 1). Background periods, apparently not affected by volcanic eruptions, occurred in 1978 to 1979 and from late 1988 to the present. The data show that the time development of the stratospheric peak aerosol mixing ratio (particles per milligram of ambient air) between these two background periods is different for the two size ranges. Although the smaller particles (radius $r \geq 0.15$ μm) do not appear to have increased in number during the past 10 years, with a background value of about 6 mg^{-1}, the background mixing ratio of the larger particles ($r \geq 0.25$ μm) has increased from about 1.1 to 1.6 mg^{-1} or about 45%. This increase, which would amount to only about 8% in the smaller size range, as it contains the larger size range as a subset, is not apparent in the small size range possibly because it is at the limit of resolution. It is also possible that a small decrease in particles with sizes between 0.15 and 0.25 μm has occurred. Because the apparent increase in background aerosol is not uniform with size, a change in the particle size distribution rather than a simple shift in concentration has apparently occurred. An investigation of this possibility requires measurements of the total aerosol concentration, which may be obtained with a condensation nuclei (CN) counter, which is sensitive to particles with radii larger than about 0.01 μm (*14*).

In contrast to the optically active component ($r \geq 0.15$ μm), the total aerosol distribution, dominated by small particles in the troposphere and at high altitude, shows a global minimum in the mixing ratio in the region of the larger sulfate (SO_4^{2-}) particles at about 18 to 22 km (*15*). This minimum is probably due to the lack of a natural source in this region and attachment to the larger particles. Measurements of CN mixing ratio profiles have been made in balloon soundings since 1974 with a thermal growth chamber attached to an optical particle counter from which the CN minimum may be determined (Fig. 2). The measurements from 1974 to 1978 are lower limits because the instrument was in a development stage, and low vapor pressure supersaturations were used in the growth chamber of the CN counter. After 1978, a counter was devel-

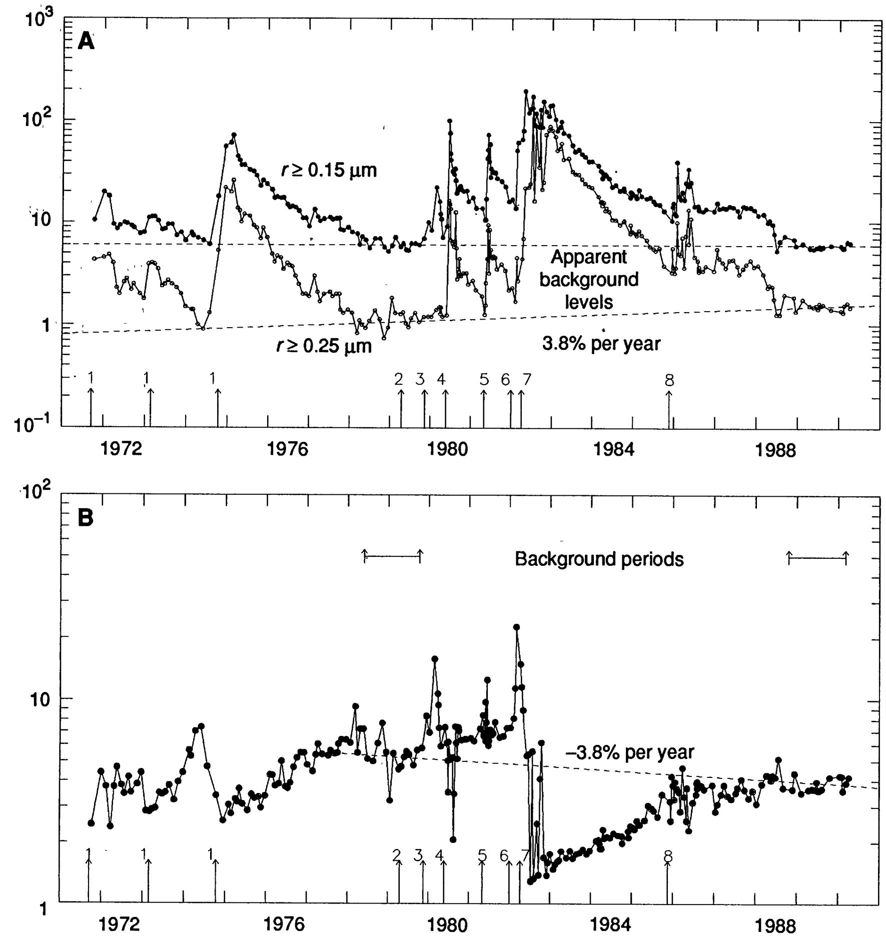

Fig. 1. (**A**) Stratospheric maximum in the aerosol mixing ratio for two size ranges and (**B**) their ratio versus time measured at Laramie, Wyoming. The dashed lines represent what are believed to be the background (nonvolcanic) levels during 1979 and 1989. Times of major volcanic eruptions are indicated: 1, Fuego; 2, La Soufriere; 3, Sierra Negra; 4, Mount St. Helens; 5, Alaid; 6, Nyamuragira; 7, El Chichon; and 8, Nevado del Ruiz.

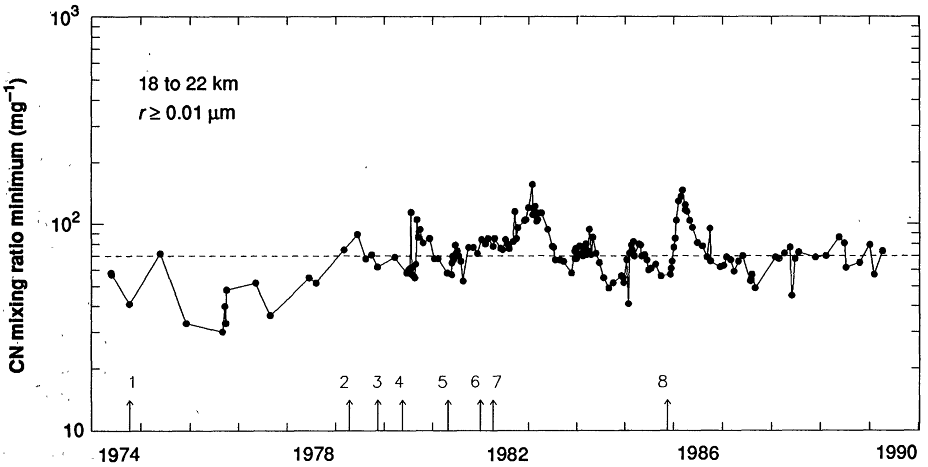

Fig. 2. The stratospheric CN mixing ratio minimum in the SO_4^{2-} layer versus time measured at Laramie, Wyoming. The dashed line represents what is believed to be the background (nonvolcanic) level, during 1979 and 1989. Times of major volcanic eruptions are as indicated in the legend to Fig. 1.

oped that used high vapor supersaturations and thus assured growth of essentially all particles present in the air sample. Except for periods after major volcanic eruptions when H_2SO_4 vapor undergoes nucleation, the nonvolcanic CN minimum at 20 km has remained relatively stable at about 70 mg^{-1} (about 6 cm^{-3}) from 1979 to 1989. These measurements further support the suggestion above that, instead of the number of particles changing, that is, a new aerosol nucleation source, the particles have become slightly larger, on the average; this change suggests that the H_2SO_4 vapor source has increased.

Because the aerosol size distribution varies with time, a parameterization is needed to determine the rate of mass increase, which is the important budget parameter. The stratospheric aerosol size distribution is most accurately described in terms of a lognormal distribution (*10*),

$$n(r)dr = \frac{N_0}{(2\pi)^{1/2}} \exp\left(-\frac{\alpha^2}{2}\right)d\alpha$$

where

$$\alpha = \frac{\ln(r/r_0)}{\ln \sigma}$$

The single-mode lognormal distribution involves three parameters: (i) the total number concentration (or mixing ratio) N_0, (ii) the distribution median radius r_0 (one half of the particles have radii greater than or less than r_0), and (iii) the distribution width σ. Typical values for the current background stratospheric aerosol layer are $N_0 = 6$ cm^{-3} or 70 mg^{-1}, $r_0 = 0.05$ µm, and $\sigma = 2.2$ ($\sigma = 1$ corresponds to a monodispersed aerosol). The total aerosol mass concentration (or mixing ratio) for spherical particles is given by

$$M = \frac{4}{3}\pi\rho N_0 r_0^3 \exp\left[\frac{9}{2}(\ln\sigma)^2\right]$$

where ρ is the aerosol specific gravity (1.65 g cm^{-3} for 75% H_2SO_4, 25% H_2O). The current mass mixing ratio of the stratospheric (20 km) background aerosol at Laramie is about 1 ppb. The integral size distribution, which is what we measure, is given by

$$N(\geq r) = \int_r^\infty n(r)dr$$

Because the size distribution involves three parameters, a measurement of the concentration at a minimum of three sizes is required. Thus, measurements of the total aerosol concentration, N_0, made with a CN counter, and of the two integral ranges $N(\geq 0.15)$ and $N(\geq 0.25)$, made with an optical particle counter, are sufficient.

The average value of N_0 in the SO_4^{2-} layer has not changed substantially since at least 1979 (Fig. 2). Unfortunately, the measurement of all three size ranges involves two instruments that were not flown together on the same balloon on a routine basis until after the eruption of Mount St. Helens in 1980. However, some data for all three size ranges were obtained on the same day during the summer of 1979. Comparison of vertical aerosol profiles obtained in soundings during the summer of 1989 and the summer of 1979 (Fig. 3) shows that, although the average lognormal median radius may have decreased slightly between 18 and 25 km, the average distribution width has increased in this region of the aerosol maximum, resulting in relatively more large

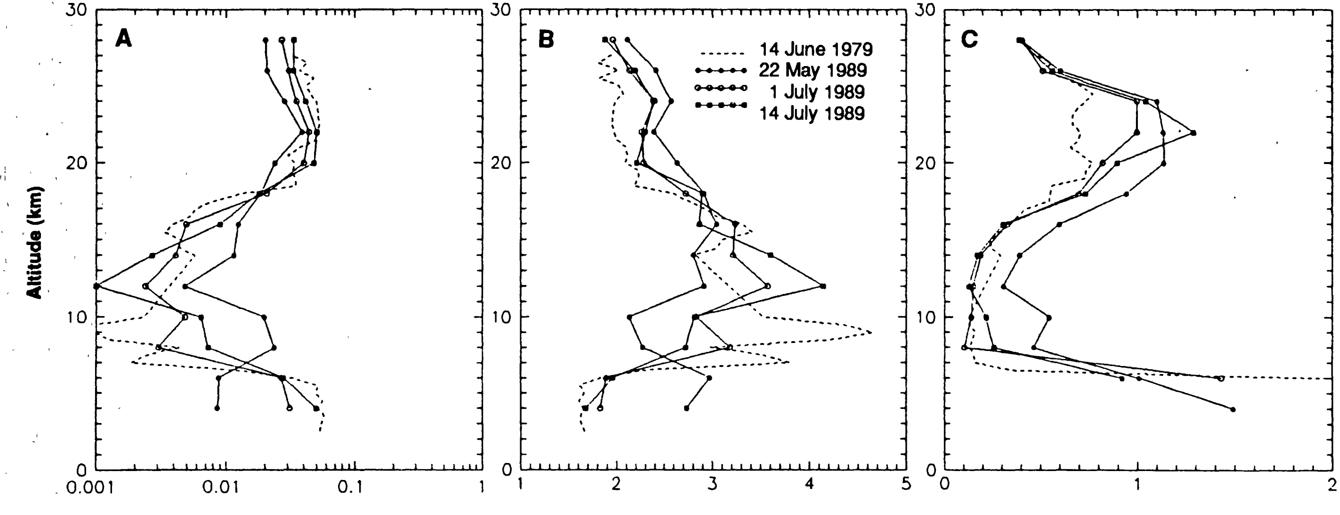

Fig. 3. (**A**) Aerosol lognormal median radius, (**B**) distribution width, and (**C**) mass mixing ratio profiles measured at Laramie, Wyoming, in mid-1989 compared to measurements in 1979.

particles and a consequent increase in the mass mixing ratio. This behavior in the parameterization is dictated by the observation of a constant total number but an increase in larger particles. Because CN concentrations vary drastically with altitude and are generally only constant with altitude and time in the CN minimum region from 18 to 22 km (where the SO_4^{2-} aerosol layer mass is maximum), these parameters are only meaningful in this altitude range. Using average values of N_0 from the CN data and $N(\geq 0.15)$ and $N(\geq 0.25)$ values of 70, 6, 1.1 mg^{-1} and 70, 6, 1.6 mg^{-1} for the 1979 and 1989 background periods, respectively, gives lognormal parameters r_0, σ, and mass mixing ratio of 0.062 μm, 1.92, 0.76 ppb and 0.052 μm, 2.24, 1.13 ppb for 1979 and 1989, respectively. This suggests a mass increase of about 5% per year. The uncertainty in measuring particle size is about 10% for spherical particles, which translates into an uncertainty in mass of about 30%. Although the relative uncertainty is smaller, because of the complicated nature of the size distribution change, we estimate a time variation of 5 ± 2% per year in the 20-km aerosol mass mixing ratio in the last 10 years.

Stratospheric aerosol levels have also been studied in Antarctica by means of annual balloon soundings at McMurdo Station (78°S) since 1972. Although these data are not as extensive as the Laramie data, changes in the stratospheric maximum in aerosol concentration at McMurdo paralleled the Laramie record. The decay of the El Chichon volcanic event in 1982 was observed there in 1983, 1984, and 1985 (*16*) and proceeded similarly to the decay observed at Laramie (Fig. 1). Little change could be detected in the stratospheric peak aerosol concentrations obtained at McMurdo during the springs of 1986 to 1989, and thus a background level appears to have been reached there by 1986. The December 1985 eruption of Nevado del Ruiz in Colombia apparently had little effect in the south polar regions.

Comparison of $r \geq 0.25$ μm aerosol concentration profiles as measured in the polar regions at McMurdo in September 1988, at Kiruna, Sweden (68°N), in January 1989, and in mid-latitudes at Laramie in February 1989 shows general agreement at the stratospheric maximum (Fig. 4), although the spring SO_4^{2-} layer is depressed in the polar regions because of winter subsidence in the cold polar vortex. The integrated column aerosol content above 12 km is 2.37×10^5, 2.20×10^5, and 2.40×10^5 cm^{-2} for McMurdo, Kiruna, and Laramie, respectively. The Laramie data were obtained with a standard particle counter, whereas the other data were obtained with a counter that had about ten times the air sample flow rate, giving better resolution (10^{-3} cm^{-3} minimum concentration as compared to 10^{-2} cm^{-3} with the standard counter). The higher resolution allowed measurement of thin polar stratospheric cloud layers, as observed in the polar soundings between 20 and 30 km (*17*).

Fig. 4. Aerosol ($r \geq 0.25$ μm) concentration profiles measured at McMurdo, Antarctica (78°S) (4 September 1988), Kiruna, Sweden (68°N) (30 January 1989), and Laramie, Wyoming (41°N) (15 February 1989).

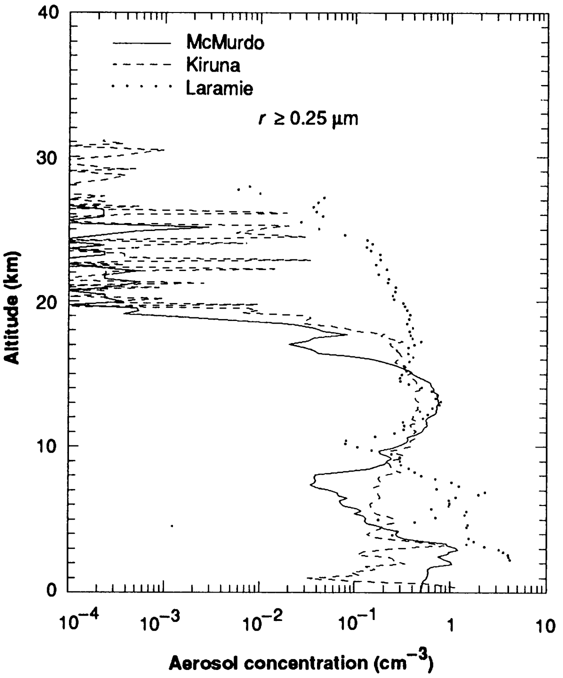

There is other evidence that particle distributions in the atmosphere are undergoing change. Aircraft sampling from 1971 to 1981 indicated that stratospheric SO_4^{2-} concentrations increased 6 to 8% per year between periods of low volcanic activity in early 1974 and 1979 (*18*). These measurements indicate that the Northern Hemisphere average SO_4^{2-} mass mixing ratio was 0.43 ppb in the summer of 1979, which is in reasonable agreement with the 1979 value we estimated when our value is reduced to account for the water in the aerosol. The stratospheric aerosol background scattering ratio (the ratio of the total amount of 694.3-nm laser light backscattered to that scattered by air molecules alone) from ground-based lidars has increased from about 1.09 to 1.10 in 1979 (*19*) to current values of about 1.2 to 1.3 (*13*). These data thus also suggest that stratospheric aerosol mass has increased. Whether this increase is natural or anthropogenic cannot be determined at this time because of inadequate information on sources, in particular, OCS, thought to be the dominant nonvolcanic source of stratospheric H_2SO_4 vapor.

Khalil and Rasmussen (*8*) estimated from budget calculations that the annual increase in OCS concentrations from anthropogenic sources was 0.6 to 0.8%, assuming that 25% of the OCS in the atmosphere was from such sources and that there was an annual increase in anthropogenic emissions of 2.5 to 3.5% from 1974 to 1979 (*8*). The 25% anthropogenic contribution was based on an interhemispheric ratio (Northern Hemisphere sources to Southern Hemisphere sources) of 1.05 derived from an OCS latitude survey conducted with aircraft from 70°N to 56°S in 1978 (*20*). However, calibration problems encountered during the survey make interpretation of the data difficult. Calculations of the anthropogenic contribution depend critically on this ratio. A ratio as high as 1.10 would make a sizable difference in these estimates (*8*).

Recent measurements suggest that the anthropogenic source of OCS may be larger than previously believed. Infrared solar occultation spectra of OCS at 28°N and 49°S, obtained with the ATMOS (atmospheric trace molecule spectroscopy) spectrometer on Spacelab 3 in 1985, indicated that the Southern Hemisphere concentrations were systematically lower than the Northern Hemisphere concentrations at all altitudes below 25 km (*5*). At 17.5 km a concentration of 500 ± 100 pptv was observed at the northern latitude, whereas at the southern latitude the value was only 300 ± 80 pptv at this altitude. Measurements in the boundary layer of the marine atmosphere between 51°N and 37°S in the Atlantic during March and April 1987 indicated relatively constant Southern Hemisphere values of OCS with an average of about 450 pptv. A pronounced increase in mixing ratio and variability was observed north of the intertropical convergence zone (≈11°N) to values as high as 800 pptv near 45°N, averaging 26 pptv per 10° of latitude and a mean hemispheric ratio of 1.25 (*21*). Furthermore, OCS concentrations correlated significantly with those of CO and CH_4. Although these results might be interpreted as indicating a seasonal variation caused by uptake of OCS by vegetation in the summer in the Southern Hemisphere, the large and variable values in the Northern Hemisphere may also be interpreted as indicating continental sources of OCS, largely anthropogenic. Additional measurements of the interhemispheric difference in OCS levels, preferably as a function of altitude, will be important in assessing the possible importance of the anthropogenic component.

In addition to possible increases in anthropogenic OCS emissions, the average global surface air temperature increase of about 0.25°C in the last 30 years (*22*) may have resulted in increased emissions from natural biogenic sulfur sources. If true, this change represents another perturbation to the global atmosphere associated with increases in greenhouse gases. In any case, a reanalysis of sulfur emission history and the stratospheric chemistry involved should be undertaken. Anthropogenic SO_2 emissions should not be overlooked; although only a few percent of surface emissions reach the stratosphere, those emissions may be 50 times that of OCS (*23*). Increased use of current air lanes near the tropopause and anticipated future use of the stratosphere for air travel present sulfur sources that could be more important than previously assumed.

REFERENCES AND NOTES

1. H. M. Steele and P. Hamill, *J. Aerosol Sci.* **12**, 517 (1981).
2. C. E. Junge, C. W. Chagnon, J. E. Manson, *J. Meteorol.* **18**, 81 (1961).
3. P. J. Crutzen, *Geophys. Res. Lett.* **3**, 73 (1976).
4. E. C. Y. Inn, J. F. Vedder, B. J. Tyson, D. O'Hara, *ibid.* **6**, 191 (1979).
5. R. Zander *et al.*, *J. Geophys. Res.* **93**, 1669 (1988).
6. O. B. Toon, R. P. Turco, P. Hamill, C. S. Kiang, R. C. Whitten, *J. Atmos. Sci.* **36**, 718 (1979).
7. R. P. Turco *et al.*, *ibid.*, p. 699.
8. M. A. K. Khalil and R. A. Rasmussen, *Atmos. Environ.* **18**, 1805 (1984).
9. D. J. Hofmann and S. Solomon, *J. Geophys. Res.* **94**, 5029 (1989).
10. D. J. Hofmann and J. M. Rosen, *ibid.* **87**, 11039 (1982).
11. ______, *Science* **208**, 1368 (1980).
12. ______, *J. Atmos. Sci.* **38**, 168 (1981).
13. *Sci. Event Alert Network (SEAN) Bull.* **13**, No. 12 (1988); *ibid.* **14**, Nos. 5, 6, 7, and 11 (1989).
14. J. M. Rosen and D. J. Hofmann, *J. Appl. Meteorol.* **16**, 56 (1977).
15. D. J. Hofmann, J. M. Rosen, W. Gringel, *J. Geophys. Res.* **90**, 2341 (1985).
16. D. J. Hofmann, J. M. Rosen, J. W. Harder, S. R. Rolf, *Geophys. Res. Lett.* **14**, 614 (1987).
17. D. J. Hofmann and T. Deshler, *ibid.* **16**, 1429 (1989).
18. W. A. Sedlacek, E. J. Mroz, A. L. Lazrus, B. W. Gandrud, *J. Geophys. Res.* **88**, 3741 (1983).
19. R. G. Pinnick *et al.*, *J. Atmos. Sci.* **33**, 304 (1976).
20. A. L. Torres, P. J. Maroulis, A. B. Goldberg, A. R. Bandy, *J. Geophys. Res.* **85**, 7357 (1980).
21. H. G. Bingemer, S. Burgermeister, R. L. Zimmermann, H.-W. Georgii, *ibid.*, in press.
22. J. F. B. Mitchell, *Rev. Geophys.* **27**, 115 (1989).
23. R. P. Turco *et al.*, *Nature* **283**, 283 (1980).

24. This research was supported by the Atmospheric Chemistry Section of the National Science Foundation.

20 November 1989; accepted 14 March 1990

Faults in the Mojave Desert, California, as Revealed on Enhanced Landsat Images

J. P. FORD, R. K. DOKKA, R. E. CRIPPEN, R. G. BLOM

Previously unknown strike-slip and normal faults in the central and eastern Mojave Desert have been revealed on Landsat Thematic Mapper images enhanced by four-component processing. This method provides color images on which lithologies are discriminated by their contrasting absorption and reflection, primarily at infrared wavelengths and particularly with regard to their ferric iron, ferrous iron, and hydroxyl contents, while retaining landform depiction. These discriminants represent a new type of geophysical display for geologic mapping in regions of well-exposed bedrock. Faults are revealed on the images by abrupt spectral and textural contrasts that coincide with aligned topographic features. The newly discovered faults form part of an extensive regional network of right shear that connects faults in the Death Valley region with the San Andreas fault system. They support a heterogeneous strain model for late Cenozoic tectonic evolution of the region. Regional structural relations indicate a westward migration of the locus of strain through time. Some of the newly identified faults bound blocks that have experienced contrasting rotational histories since early Miocene time.

THE MOJAVE DESERT BLOCK (MDB) tectonic unit in Southern California has had a complex history of late Cenozoic deformation. The block covers ~38,000 km^2 at the western margin of the North American Plate. It is bounded by the San Andreas fault zone to the southwest, the Pinto Mountain fault to the south, the Garlock fault to the north, and the Granite Mountains fault to the east (*1*) (Fig. 1). The MDB is thought to have been deformed under two different tectonic regimes in late Cenozoic time. Early Miocene extensional tectonism in the Mojave (*2, 3*) was followed by dominantly northwest-striking, right-slip faulting that began after 13 Ma (million years ago) (*1, 4*). Paleomagnetic evidence suggests that both regimes were accompanied by block rotations (*5–7*). The MDB is broken internally by many subparallel strike-slip faults 10 to 20 km apart. Dibblee (*8*) recognized the right-slip character of these faults and their likely relationship to the San Andreas fault system. Subsequent tectonic models held that the faults resulted from simple shear that was regionally distributed across the MDB in late Cenozoic time, but the details of timing and fault development were not well understood (*9*). These faults are important because of their dominant role in establishing the present structural and physiographic grain of the MDB and for the seismic hazard that they represent (*10*).

About 50% of the surface area of the MDB consists of alluviated basins and associated dry lake beds (*11*). Although vegetative cover is sparse (<10%), the geology of the basins and alluviated surfaces is poorly known and largely generalized on the basis of reconnaissance mapping (1:62,500 or smaller). One reason is that much of the MDB is difficult of access or is closed to the public. Also, alluvium and dry lake deposits cover the bedrock geology in key areas. Images obtained at multiple wavelengths by the earth-orbiting Landsat Thematic Mapper (TM) system are suitable for regional and local analyses and provide map scale data that are not available from other sources.

We have used Landsat TM, aerial photographs, and other types of images to study ~2000 km^2 in the central and eastern MDB, where little detailed mapping is available. Landsat TM images processed by a four-component technique have provided valuable spectral information that reveals contrasting compositional characteristics of the rocks mostly at infrared wavelengths, while retaining landform depiction. Such

---

J. P. Ford, R. E. Crippen, R. G. Blom, Jet Propulsion Laboratory, Mail Stop 300/233, Pasadena, CA 91109.
R. K. Dokka, Louisiana State University, Department of Geology and Geophysics, Baton Rouge, LA 70803.